

## A change of the Fermi surface in $\text{UGe}_2$ across the critical pressure

This article has been downloaded from IOPscience. Please scroll down to see the full text article.

2002 J. Phys.: Condens. Matter 14 L29

(<http://iopscience.iop.org/0953-8984/14/1/104>)

View [the table of contents for this issue](#), or go to the [journal homepage](#) for more

Download details:

IP Address: 171.66.16.238

The article was downloaded on 17/05/2010 at 04:42

Please note that [terms and conditions apply](#).

## LETTER TO THE EDITOR

## A change of the Fermi surface in UGe<sub>2</sub> across the critical pressure

R Settai<sup>1,6</sup>, M Nakashima<sup>1</sup>, S Araki<sup>1</sup>, Y Haga<sup>2</sup>, T C Kobayashi<sup>3</sup>,  
N Tateiwa<sup>4</sup>, H Yamagami<sup>5</sup> and Y Ōnuki<sup>1,2</sup>

<sup>1</sup> Graduate School of Science, Osaka University, Toyonaka, Osaka 560-0043, Japan

<sup>2</sup> Advanced Science Research Center, Japan Atomic Energy Research Institute, Tokai, Ibaraki 319-1195, Japan

<sup>3</sup> Research Center for Materials Science at Extreme Conditions, Osaka University, Toyonaka, Osaka 560-8531, Japan

<sup>4</sup> Graduate School of Engineering Science, Osaka University, Toyonaka, Osaka 560-8531, Japan

<sup>5</sup> Faculty of Science, Department of Physics, Kyoto Sangyo University, Kita-ku, Kyoto 603-8555, Japan

E-mail: settai@phys.sci.osaka-u.ac.jp

Received 18 October 2001, in final form 31 October 2001

Published 7 December 2001

Online at [stacks.iop.org/JPhysCM/14/L29](http://stacks.iop.org/JPhysCM/14/L29)

### Abstract

We carried out the de Haas–van Alphen (dHvA) experiment under pressure for a ferromagnet UGe<sub>2</sub>. The dHvA frequency of a main dHvA branch named  $\alpha$ , that corresponds to a majority up-spin band 40-hole Fermi surface, decreases monotonously with increasing pressure, but in the pressure range from  $p_c^*$  ( $\simeq 1.2$  GPa) to  $p_c$  ( $\simeq 1.5$  GPa) the dHvA signal disappears completely, where  $p_c$  and  $p_c^*$  correspond to critical pressures for a Curie temperature  $T_C$  and the second phase transition temperature  $T^*$  ( $< T_C$ ), respectively. For  $p > p_c$  we observed new dHvA branches with large cyclotron masses of 19–64 $m_0$ , which correspond to main Fermi surfaces in the paramagnetic state.

The coexistence of superconductivity with magnetism is an important issue in condensed-matter physics [1]. In f-electron systems, superconductivity was observed in a quantum critical region where the Néel temperature of antiferromagnets such as CeIn<sub>3</sub> and CePd<sub>2</sub>Si<sub>2</sub> became zero [2]. Surprisingly superconductivity was recently observed in a ferromagnet UGe<sub>2</sub> with the Curie temperature  $T_C = 52$  K [3]. This is the first example where superconductivity truly coexists with strong ferromagnetism with a magnetic moment  $1 \mu_B/U$  [4].

UGe<sub>2</sub> crystallizes in the orthorhombic crystal structure of *Cmmm* ( $a = 4.0089$  Å,  $b = 15.0889$  Å and  $c = 4.0950$  Å) with a large lattice constant along the  $b$ -axis [5]. The crystal structure possesses inversion symmetry, which is needed for odd-parity superconductivity [1].

<sup>6</sup> To whom correspondence should be addressed.

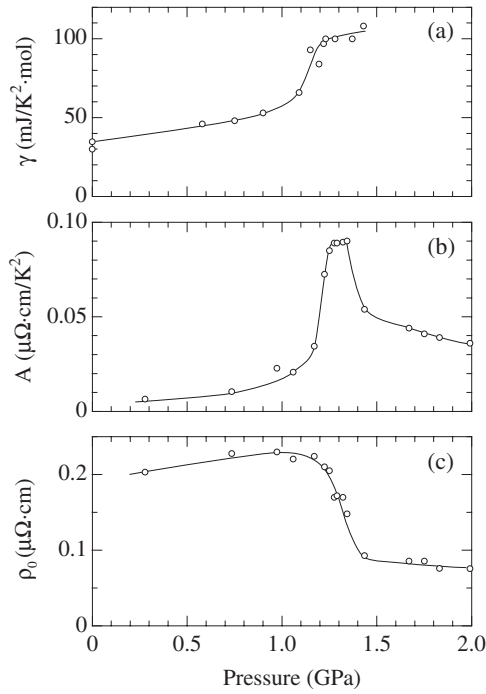


**Figure 1.** Pressure dependence of the (a)  $\gamma$ , (b)  $A$  and (c)  $\rho_0$  values in  $\text{UGe}_2$ .

It is noted that the crystal structure  $Cmcm$  was adopted in the literature before 1996. The  $a$ - and  $c$ -axes in  $Cmcm$  should be changed into the  $c$ - and  $a$ -axes in  $Cmmm$ , respectively.

Reflecting the characteristic crystal structure, the magnetic property is also highly anisotropic [6, 7]. The ordered moment  $\mu_s$  is  $1.4 \mu_B/\text{U}$ , directed along the  $a$ -axis. The  $b$ - and  $c$ -axes are hard axes, indicating strong anisotropy. The main Fermi surfaces, which were determined by the de Haas–van Alphen (dHvA) experiment and energy-band calculations, are nearly cylindrical along the  $b$ -axis [8–10]. The corresponding cyclotron masses are relatively large, i.e.  $15\text{--}20m_0$ . It was concluded that the 5f electrons in  $\text{UGe}_2$  are itinerant, indicating band magnetism as in 3d-electron systems.

In the pressure experiment, it was clarified that with increasing pressure  $p$ ,  $T_C$  becomes zero roughly at  $p_c \simeq 2$  GPa [11]. The second phase transition was later found below  $T_C$ , at  $T^* \simeq 30$  K at ambient pressure [12, 13].  $T^*$  also becomes zero at  $p_c^* \simeq 1$  GPa. Around  $p_c^*$ , namely in the pressure region from 1.0 to 1.6 GPa superconductivity was observed below 0.7 K [3, 4]. This superconductivity is bulk natured as confirmed by the specific-heat experiment [14]. Superconductivity is realized within the ferromagnetic region centred at  $p_c^*$  and disappears in the paramagnetic state ( $p > p_c$ ), strongly suggesting that superconductivity is mediated by the magnetic origin instead of by phonons in conventional superconductors.

As shown in figure 1, obtained recently from resistivity and specific-heat experiments, the  $A$  value of the electrical resistivity  $\rho (= \rho_0 + AT^2)$  has a peak at about 1.3 GPa. The corresponding electronic specific-heat coefficient  $\gamma$  reaches  $100 \text{ mJ K}^{-2} \text{ mol}^{-1}$ . The residual resistivity  $\rho_0$  increases almost linearly as the pressure increases but decreases steeply above 1.2 GPa, reaching an extremely low residual resistivity in the paramagnetic state. Here,  $p_c^*$  and  $p_c$  are considered to be to 1.2 and 1.6 GPa, respectively.

To further clarify the Fermi-surface property, we carried out the dHvA experiment under pressure. We found a drastic change in the Fermi surface when the pressure crossed  $p_c$ .

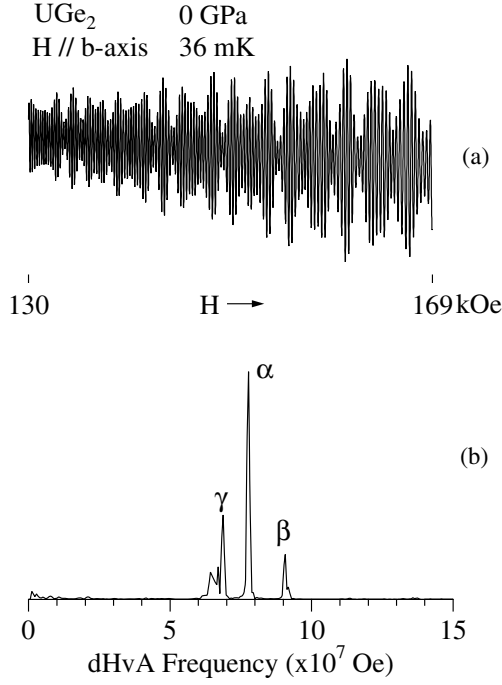


**Figure 2.** (a) dHvA oscillation and (b) the corresponding FFT spectrum at ambient pressure in  $\text{UGe}_2$ .

A single crystal was almost the same as in [14], grown by the Czochralski pulling method and annealed in high vacuum. The dHvA experiment was done by the standard field modulation method in magnetic fields up to 170 kOe and at low temperatures down to 30 mK. The pressure experiment was carried out using a MP35N piston-cylinder cell. The pressure-transmitting medium was a 1:1 mixture of commercial Daphne oil (7373) and kerosene.

Figure 2 shows the typical dHvA oscillation and the corresponding fast Fourier transformation (FFT) spectrum for the field along the  $b$ -axis at ambient pressure (0 GPa). The dHvA frequencies of  $(6.5\text{--}9.2) \times 10^7$  Oe correspond to the main Fermi surfaces, where the dHvA frequency  $F(= (c\hbar/2\pi e)S_F)$  is proportional to the maximum or minimum cross sectional area  $S_F$  of the Fermi surface.

Fermi surfaces were calculated in the scheme of a fully-relativistic spin-polarized version of the linearized augmented-plane-wave (LAPW) method [15] within a local spin-density approximation under the assumption that 5f electrons are itinerant and the magnetic moment is directed along the  $a$ -axis. Band 40-hole and 41-electron Fermi surfaces in figure 3 correspond to majority up-spin bands, while minority down-spin states are included partially in band 39-hole and 42-electron Fermi surfaces. In the present band calculations, a magnetic moment of  $1.2 \mu_B/U$  was obtained, with spin and orbital moments  $-1.3$  and  $2.5 \mu_B/U$ , respectively.

Branch  $\alpha$  with dHvA frequency  $F = 7.76 \times 10^7$  Oe and the cyclotron mass  $m_c^* = 15m_0$  in figure 2 most likely corresponds to an outer orbit of the majority up-spin band 40-hole Fermi surface with a calculated dHvA frequency of  $5.14 \times 10^7$  Oe and the band mass  $m_b = 9.08m_0$ . The detected dHvA frequency (and cyclotron mass) in figure 2 are  $9.06 \times 10^7$  Oe ( $18m_0$ ) for branch  $\beta$  and  $6.86 \times 10^7$  Oe ( $23m_0$ ) for branch  $\gamma$ , which are also identified as the band-40 hole ( $10.53 \times 10^7$  Oe,  $11.11m_0$ ) and the band 41-electron ( $6.81 \times 10^7$  Oe,  $17.78m_0$ ), respectively. Here the cyclotron mass was determined by the temperature dependence of the dHvA amplitude.

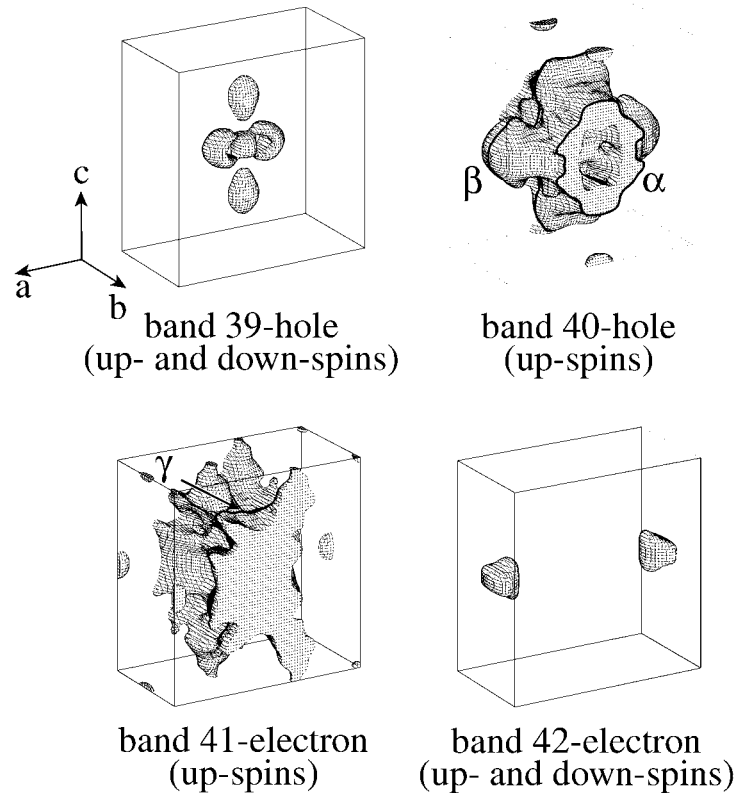


**Figure 3.** Fermi surfaces in the ferromagnetic state of  $\text{UGe}_2$ .

On increasing the pressure, the dHvA frequency of branch  $\alpha$  becomes smaller. The dHvA signal, however, disappears completely in the pressure range from 1.2 to 1.5 GPa. In the paramagnetic region we observed a new dHvA oscillation. Figure 4 shows the dHvA oscillation and its FFT spectrum at 1.82 GPa. The dHvA branches are named A, B, C and D, where the corresponding dHvA frequencies (and cyclotron masses) are  $8.02 \times 10^7$  ( $43m_0$ ),  $7.20 \times 10^7$  ( $57m_0$ ),  $8.40 \times 10^7$  ( $64m_0$ ) and  $1.59 \times 10^7$  Oe ( $19m_0$ ), respectively.

Figure 5 indicates the FFT spectra at various pressures. The FFT spectra are very different below and above about 1.5 GPa ( $\simeq p_c$ ). In the present dHvA experiment we obtained no dHvA signal at 1.50 GPa but a clear signal at 1.54 GPa. The  $p_c$  value is close to 1.5 GPa rather than 1.6 GPa.

We show in figure 6 the pressure dependence of the dHvA frequency and the cyclotron effective mass. The dHvA frequency of branch  $\alpha$ , together with that of branch  $\beta$ , decreases almost linearly with increasing pressure. The cyclotron mass of  $15m_0$  for branch  $\alpha$  at ambient pressure increases up to  $22m_0$  at 1.18 GPa with a tendency of a steep increase above  $p_c^* \simeq 1.2$  GPa. The cyclotron mass in the paramagnetic state is surprisingly large: 43, 57, 64 and  $19m_0$  at 1.82 GPa for branches A, B, C and D, respectively. The cyclotron mass in the paramagnetic state has a tendency to decrease as the pressure increases, which is approximately consistent with the A value in figure 1(b).

We will discuss a change of the Fermi surface under pressure. A characteristic pressure region is classified into three regions: (1)  $p < p_c^*$ , (2)  $p_c^* < p < p_c$  and (3)  $p > p_c$ . In

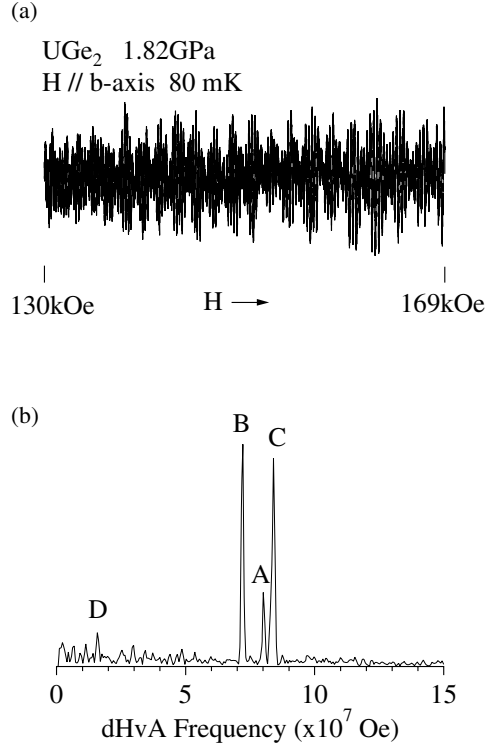


**Figure 4.** (a) dHvA oscillation and (b) the corresponding FFT spectrum at 1.82 GPa in UGe<sub>2</sub>.

the first pressure region of  $p < p_c^*$ , the dHvA frequency of branch  $\alpha$ , which most likely corresponds to the majority up-spin band 40-hole Fermi surface, decreases almost linearly with increasing pressure. This means that a volume of the majority up-spin band 40-hole Fermi surface decreases as the pressure increases. Correspondingly, the Curie temperature  $T_C$  decreases from 52 K at ambient pressure to about 30 K at  $p_c^*$ , and an ordered moment decreases from 1.45 to about  $1.0 \mu_B/U$  [4]. Simply put, it is expected that as the pressure increases the volumes of both the band 40-hole and band 41-electron Fermi surfaces with majority up-spin states decrease, while the volumes of both the band 39-hole and the band 42-electron Fermi surfaces with minority down-spin states increase correspondingly. Note that both the up- and down-spin states are involved in the band 39-hole and band 42-electron Fermi surfaces at ambient pressure. The ordered moment, which is proportional to a volume difference between Fermi surfaces with up- and down-spin states, thus decreases as the pressure increases. Experimentally we have, however, found no direct evidence for the Fermi surface with the down-spin state. The dHvA frequency of  $7.12 \times 10^7$  Oe was observed at 1.18 GPa. It is unclear whether this branch corresponds to the Fermi surface with minority down-spin states.

Next we will discuss the electronic state in the second pressure region of  $p_c^* < p < p_c$ . In this pressure region the dHvA signal disappears completely. There are a few reasons for this. One is a large  $\gamma$  value in this region. The  $\gamma$  value reaches  $100 \text{ mJ K}^{-2} \text{ mol}^{-1}$ , as shown in figure 1(a), which is much larger than  $35 \text{ mJ K}^{-2} \text{ mol}^{-1}$  at ambient pressure. A large effective mass of the conduction electron reduces intensively the dHvA amplitude. Another is a large residual resistivity in this region, as shown in figure 1(c). In other words, a small residual resistivity in the paramagnetic state is why the dHvA signal was observed

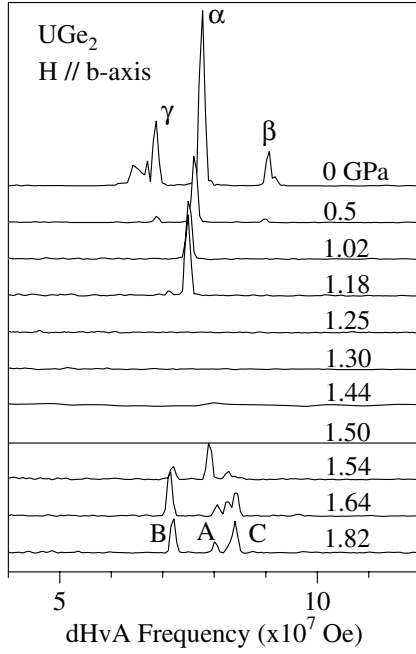


**Figure 5.** FFT spectra at various pressures in UGe<sub>2</sub>.

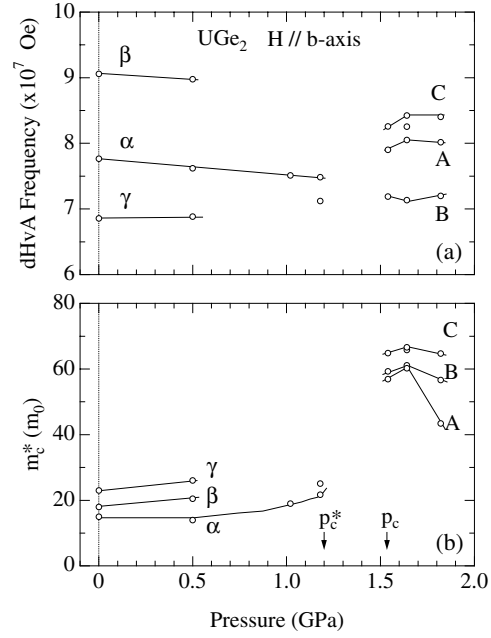


**Figure 6.** Pressure dependence of (a) the dHvA frequency and (b) the cyclotron mass in UGe<sub>2</sub>.

for carriers with large cyclotron masses of 19–64 $m_0$  at 1.82 GPa, in the third pressure region of  $p > p_c$ . Usually the ferromagnetic order does not cause a scattering at low temperatures because spins are oriented uniformly in one direction. The second phase transition at  $T^*$  might bring about strong scattering for conduction electrons. It is pointed out that the second phase transition corresponds to a charge density wave (CDW) and/or a spin density wave (SDW) formation [4], although experimental evidence has not yet been observed for neutron scattering. If the CDW/SDW state is formed below  $T^*$ , it will also bring about a slight change in the Fermi surface. Experimentally the magnetic moment is enhanced below  $T^*$  [4, 16], which corresponds to a change in the Fermi surface. We note that a new mechanism of unconventional superconductivity is theoretically proposed on the basis of CDW/SDW fluctuations [17].

In the paramagnetic state we observed a clear dHvA oscillation. Branches A, B, C and D are approximately identified in theoretical Fermi surfaces in figure 7, which were calculated using the lattice parameter at ambient pressure in the paramagnetic state. As shown in figure 7, UGe<sub>2</sub> is a compensated metal because it possesses two molecules in the primitive cell. Band 19- and 20-hole Fermi surfaces are compensated by a band 21-electron Fermi surface, and up- and down-spin states are degenerated in the paramagnetic state. Four kinds of theoretical dHvA frequencies corresponding to branches A, B, C and D are :  $9.21 \times 10^7$  (8.74 $m_0$ ),  $5.00 \times 10^7$  (12.2 $m_0$ ),  $11.7 \times 10^7$  (14.2 $m_0$ ) and  $0.38 \times 10^7$  Oe (6.01 $m_0$ ), respectively. These dHvA frequencies are quantitatively not in good agreement with the experimental values, although a rough correspondence between the theory and the experiment is obtained. This discrepancy is mainly due to low symmetry of the orthorhombic crystal structure.

In the pressure region of  $1.0 < p < 1.6$  GPa, superconductivity was observed [3, 4, 14]. We also confirmed superconductivity from the ac-susceptibility measurement using the detecting coil in the present dHvA experiment: 0.03 K at 1.02 GPa, 0.70 K at 1.18 GPa and

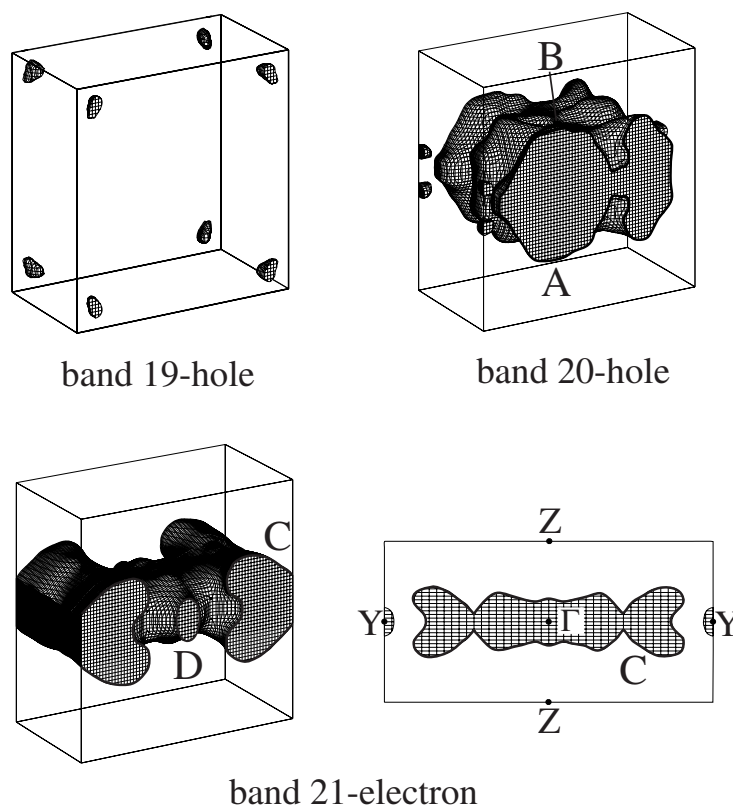


**Figure 7.** Fermi surfaces in the paramagnetic state of  $\text{UGe}_2$ .

0.20 K at 1.50 GPa, but no superconductivity down to 40 mK at 1.54 GPa. In this pressure region of  $1.0 < p < 1.6$  GPa, the magnetic moment is intensively reduced [4, 16]. Correspondingly the volume of the Fermi surface with majority up-spin states decreases and inversely the volume of the Fermi surface with minority down-spin states is expected to increase. Moreover the second phase transition might change the Fermi surface. This electronic state in the pressure region of  $1.0 < p < 1.6$  GPa possesses a large  $\gamma$  value of  $100 \text{ mJ K}^{-2} \text{ mol}^{-1}$ , and unconventional superconductivity with the triplet pairing mechanism is most likely realized in this pressure region [17, 18]. Unfortunately we could not gain information on the Fermi surface in  $p_c^* (\simeq 1.2 \text{ GPa}) < p < p_c (\simeq 1.5 \text{ GPa})$ , although a drastic change in the Fermi surface was clearly indicated above  $p_c$  in the present dHvA experiment.

The authors are grateful to Professor K Miyake for helpful discussions. This work was supported by the Grant-in-Aid for Scientific Research COE (10CE2004) from the Ministry of Education, Culture, Science, Sports and Technology.

## References

- [1] Sigrist M and Ueda K 1991 *Rev. Mod. Phys.* **63** 239
- [2] Mathur N D, Grosche F M, Julian S R, Walker I R, Freye D M, Haselwimmer R K W and Lonzarich G G 1998 *Nature* **394** 39



- 
- [3] Saxena S S *et al* 2000 *Nature* **604** 587
- [4] Huxley A, Shikin I, Ressouche E, Kernavanois N, Braithwaite D, Calemczuk R and Flouquet J 2001 *Phys. Rev. B* **63** 144519
- [5] Oikawa K, Kamiyama T, Asano H, Ōnuki Y and Kohgi M 1996 *J. Phys. Soc. Japan* **65** 3229
- [6] Menovsky A, de Boer F R, Frings P H and Franse J J M 1983 *High Field Magnetism* ed M Date (Amsterdam: North-Holland) p 189
- [7] Ōnuki Y, Ukon I, Yun S W, Umehara I, Satoh K, Fukuhara T, Sato H, Takayanagi H, Shikama M and Ochiai A 1992 *J. Phys. Soc. Japan* **61** 293
- [8] Satoh K, Yun S W, Umehara I, Ōnuki Y, Uji S, Shimizu T and Aoki H 1992 *J. Phys. Soc. Japan* **61** 1827
- [9] Yamagami H and Hasegawa A 1993 *Physica B* **186–8** 182
- [10] Shick A B and Pickett W E 2001 *Phys. Rev. Lett.* **8** 300
- [11] Takahashi H, Mōri N, Ōnuki Y and Yun S W 1993 *Physica B* **186–8** 772
- [12] Oomi G, Nishimura K, Ōnuki Y and Yun S W 1993 *Physica B* **186–8** 758
- [13] Oomi G, Kagayama T, Nishimura K, Yun S W and Ōnuki Y 1995 *Physica B* **206/207** 515
- [14] Tateiwa N, Kobayashi T C, Hanazono K, Amaya K, Haga Y, Settai R and Ōnuki Y 2001 *J. Phys.: Condens. Matter* **L17**
- [15] Yamagami H 1998 *J. Phys. Soc. Japan* 3176  
Yamagami H 2000 *Phys. Rev. B* **61** 6264
- [16] Tateiwa N, Hanazono K, Kobayashi T C, Amaya K, Inoue T, Kindo K, Koike Y, Metoki N, Haga Y, Settai R and Ōnuki Y 2001 *J. Phys. Soc. Japan* **70** 2876
- [17] Watanabe S and Miyake K 2001 *SCES* submitted  
Watanabe S and Miyake K 2001 *Physica* at press
- [18] Machida K and Ohmi T 2001 *Phys. Rev. Lett.* **86** 850